

Itinerant ferromagnetism with finite ranged interactions

C.W. von Keyserlingk¹ and G.J. Conduit^{2,*}

¹*Rudolf Peierls Centre for Theoretical Physics, 1 Keble Road, Oxford, OX1 3NP, United Kingdom*

²*Cavendish Laboratory, J.J. Thomson Avenue, Cambridge, CB3 0HE, United Kingdom*

(Dated: March 11, 2022)

Quantum fluctuations are of central importance in itinerant ferromagnets; in the case of the Stoner Hamiltonian, with contact interactions, they deliver a rich phase diagram featuring a first order ferromagnetic transition preempted by a spin spiral and a paired density wave. However, to date all analyses of fluctuation corrections neglect the finite ranged nature of the Coulomb interaction. We develop the formalism to consider the effects of fluctuations with a realistic screened Coulomb potential. The finite ranged interaction suppresses the tricritical point temperature of the first order ferromagnetic transition, bringing theory into line with experiment, whilst retaining the exotic spin spiral and paired density wave. In an ultracold atomic gas a finite ranged interaction damps the competing molecular instability, permitting the observation of ferromagnetic correlations.

PACS numbers: 03.75.Ss, 71.10.Ca, 67.85.-d

Metallic systems in the vicinity of second order phase transitions display remarkable quantum critical phenomena [1]. However, in several metals [2–6] quantum criticality gives way to a first order transition, spatially modulated magnetic order [7–9], and a p-wave superconducting instability [10–14]. Starting from a minimal Hamiltonian of freely dispersing electrons with a repulsive contact interaction, theory indicates that soft magnetic fluctuations transverse to the magnetic order drive the first order transition [15–21], spin spiral phase [15], and the p-wave superconducting instability [22]. However, there is a significant discrepancy: experiments typically show a tricritical temperature of $T_c \approx 0.02T_F$ [8, 9, 23] (in $\text{Sr}_3\text{Ru}_2\text{O}_7$), while theory predicts $T_c \approx 0.3T_F$ [15]. Here we demonstrate both analytically and numerically that this discrepancy can be resolved by using the realistic screened Coulomb potential rather than the ubiquitous contact potential.

A cold atom gas presents an alternative forum to explore the Stoner Hamiltonian. Attempts to observe itinerant ferromagnetism in a cold atom gas have been thwarted [24–30] by a competing instability to a molecular bound state [31]. Motivated by the suppression of pairing in a narrow Feshbach resonance [32, 33], here we demonstrate how a finite interaction range removes pairing in a region of stable ferromagnetic order.

In this paper we study itinerant ferromagnetism in the presence of a finite ranged repulsive interaction. We extend an analytical fluctuation correction formalism that has already delivered a phase diagram containing a first order ferromagnetic phase transition [16], spiral phase [15], and p-wave superconducting instability [22] to now include a finite ranged interaction and calculate the phase diagram. Second, we perform complementary Quantum Monte Carlo calculations to verify the zero temperature behavior. Finite ranged interactions suppress the tricritical point temperature. Finally, we focus on the cold atom gas with finite ranged interactions

that displays ferromagnetic order whilst circumventing the competing pairing process.

FORMALISM

To study itinerant ferromagnetism in the presence of a finite ranged interaction we focus on the idealized Hamiltonian

$$\hat{H} = \sum_{\mathbf{p}, \sigma \in \{\uparrow, \downarrow\}} \xi_{\mathbf{p}\sigma} c_{\mathbf{p}, \sigma}^\dagger c_{\mathbf{p}, \sigma} - \sum_{\mathbf{p}\uparrow, \mathbf{p}\downarrow, \mathbf{q}} g(\mathbf{p}\uparrow - \mathbf{p}\downarrow, \mathbf{q}) c_{\mathbf{p}\uparrow - \mathbf{q}/2, \uparrow}^\dagger c_{\mathbf{p}\downarrow + \mathbf{q}/2, \downarrow}^\dagger c_{\mathbf{p}\downarrow - \mathbf{q}/2, \downarrow} c_{\mathbf{p}\uparrow + \mathbf{q}/2, \uparrow}, \quad (1)$$

where $\xi_{\mathbf{p}} = p^2/2 - \mu$ is the dispersion, μ is the chemical potential, and we adopt atomic units $\hbar = m = k_B = 1$. A general momentum dependent interaction $g(\mathbf{p}, \mathbf{q})$ acts between the two species, where \mathbf{p} is the incoming relative momentum and \mathbf{q} represents the momentum transfer. The Stoner Hamiltonian of electrons interacting with a contact interaction would be recovered with $g(\mathbf{p}, \mathbf{q}) = g$. To study the onset of ferromagnetic order, two *ab initio*, complementary, and mutually consistent tools have emerged: the analytical order by disorder approach [16], and Quantum Monte Carlo [15, 34]. We now extend both methods to probe and understand the consequences of finite range interactions.

Functional integration

The functional integral formalism calculates the quantum partition function expressed as a coherent state field

	Solid state $g(\mathbf{p}, \mathbf{q})/g =$	Separable cold atoms $g(\mathbf{p}, \mathbf{q})/g =$	Reciprocal cold atoms $g(\mathbf{p}, \mathbf{q})/g =$
Functional	$(1 + b^2 q^2)^{-1}$	$1 + 2ar_e(p^2 + q^2)$	$[1 - 2ar_e(p^2 + q^2)]^{-1}$
Mean-field	1	$1 + \frac{12}{5}k_F a k_F r_e$	Numerical
Fluctuation	$(1 + 2k_F^2 b^2)^{-1}$	$1 + 8k_F a k_F r_e$	$(1 - 8k_F a k_F r_e)^{-1}$
MF trans.	$g\nu_F = 1$	$k_F a = \frac{\pi}{2} - \frac{3\pi^2 k_F r_e}{5}$	Numerical

TABLE I. The rescaling of the interaction strength in the mean-field and fluctuation contributions to the free energy on introducing finite range interactions for the solid state and cold atoms cases. The bottom row shows the expected interaction strength of the magnetic transition in the mean-field approximation.

integral

$$\mathcal{Z} = \int \mathcal{D}\psi \exp \left[- \sum_{p, \sigma = \{\uparrow, \downarrow\}} \bar{\psi}_{p, \sigma} (-i\omega + \xi_{\mathbf{p}\sigma}) \psi_{p, \sigma} - \sum_{p \uparrow, p \downarrow, q} g(\mathbf{p} \uparrow - \mathbf{p} \downarrow, \mathbf{q}) \bar{\psi}_{p \uparrow - q/2, \uparrow} \bar{\psi}_{p \downarrow + q/2, \downarrow} \psi_{p \downarrow - q/2, \downarrow} \psi_{p \uparrow + q/2, \uparrow} \right], \quad (2)$$

where the field ψ describes a two component Fermi gas. We use the four-momentum notation $p = \{\omega, \mathbf{p}\}$ with Matsubara frequencies ω and inverse temperature $\beta = 1/T$.

We decouple the quartic interaction term with a Hubbard-Stratonovich transformation into the full vector magnetization ϕ and density channel ρ [16]. This decoupling scheme is sensitive to the spin spiral instability driven by transverse magnetic fluctuations, and simultaneously the p-wave superconducting instability driven by longitudinal magnetic fluctuations. The action is now quadratic in the Fermionic degrees of freedom, and after integrating them out we recover the quantum partition function $\mathcal{Z} = \int \mathcal{D}\phi \mathcal{D}\rho \exp(-S)$ with an action

$$S = \text{Tr} [\phi \hat{g} \phi - \rho \hat{g} \rho] - \text{Tr} \ln \left[(\hat{\partial}_\tau + \hat{\xi}_\alpha + \hat{g} \rho) \mathbf{I} - \hat{g} \phi \cdot \boldsymbol{\sigma} \right], \quad (3)$$

where \hat{g} is the operator form of the potential. We expand the action to quadratic order in fluctuations of ρ and ϕ around their putative saddle-point values ρ_0 and $\mathbf{M}_\mathbf{Q} = M(\cos \mathbf{Q} \cdot \mathbf{r}, \sin \mathbf{Q} \cdot \mathbf{r}, 0)$, where \mathbf{Q} is the spiral wave vector. A gauge transformation renders the magnetization uniform and modifies the dispersion as $\xi_{\mathbf{p}\sigma} = p^2/2 + \sigma \sqrt{(\mathbf{p} \cdot \mathbf{Q})^2 + (gM)^2} - \mu$. After integrating over magnetization and density fluctuations the free energy is

$$F = \sum_{\mathbf{p}, \sigma} \frac{p^2}{2m_\sigma} n(\xi_{\mathbf{p}\sigma}) + \sum_{\mathbf{p} \uparrow, \mathbf{p} \downarrow} g(\mathbf{p} \uparrow - \mathbf{p} \downarrow, \mathbf{0}) n(\xi_{\mathbf{p} \uparrow}) n(\xi_{\mathbf{p} \downarrow}) - \sum_{\substack{\mathbf{p}_1 + \mathbf{p}_2 \\ = \mathbf{p}_3 + \mathbf{p}_4}} g(\mathbf{p}_1 - \mathbf{p}_3, \mathbf{p}_1 - \mathbf{p}_4)^2 \frac{n(\xi_{\mathbf{p}_1 \uparrow}) n(\xi_{\mathbf{p}_2 \downarrow}) [n(\xi_{\mathbf{p}_3 \uparrow}) + n(\xi_{\mathbf{p}_4 \downarrow})]}{\xi_{\mathbf{p}_1 \uparrow} + \xi_{\mathbf{p}_2 \downarrow} - \xi_{\mathbf{p}_3 \uparrow} - \xi_{\mathbf{p}_4 \downarrow}}.$$

The first term is the kinetic energy, the second the mean-field contribution of the interactions, and the third is the fluctuation correction. The momentum summation in the mean-field term introduces a weighted average that can be performed analytically for certain potentials at low temperature. The momentum summation in the fluctuation term is dominated by the contributions at $p^2 + q^2 = 4k_F^2$ [15] and therefore the interaction potential can be approximated by $g(\mathbf{p}, \mathbf{q}) \mapsto g(\sqrt{2}k_F, \sqrt{2}k_F)$. These two observations allow us to simply rescale the interaction strength that appears in the mean-field and fluctuation correction terms and afterwards treat them as pure contact interactions. The validity of the approximation will be verified in the cold atom section.

We now enumerate the interaction potentials that we adopt for describing the solid state and cold atom gas.

Solid state: We use the Coulomb interaction $ge^{-r/b}/4\pi b^2 r$ with screening length b , whose Fourier transform $g(\mathbf{p}, \mathbf{q}) = g/(1 + b^2 q^2)$ depends only on the momentum transfer \mathbf{q} .

Cold atoms: The T-matrix that describes the Feshbach resonance can be modeled by several potentials [15, 35, 36]. Here we concentrate on two: the separable form used by Pekker that facilitates the momentum summation [32, 33]; $g(\mathbf{p}, \mathbf{q}) = (2k_F a / \pi \nu_F) [1 + 2ar_e(p^2 + q^2)]$; and to establish a direct contact with the screened Coulomb interaction a reciprocal form (a Taylor expansion of the former) $g(\mathbf{p}, \mathbf{q}) = (2k_F a / \pi \nu_F) / [1 - 2ar_e(p^2 + q^2)]^{-1}$. Both potentials depend on the energy in the center-of-mass frame that appears in the scattering amplitude. Here the interaction strength is analogous to the scattering length $k_F a$, the effective range is r_e , and ν_F is the density of states at the Fermi surface.

In Table (I) we summarize how the interaction potentials rescale the mean-field and fluctuation correction potentials after performing the momentum summations.

Quantum Monte Carlo

The fluctuation corrections included in the analytical formalism represent a subset of all possible contributions to the free energy. To gauge the effectiveness of our analytical formalism we perform Diffusion Monte Carlo calculations with the CASINO program [37]. The approach is a refinement of that used in previous studies of itinerant ferromagnetism [15, 34, 38]. This method optimizes a trial wave function at zero temperature to yield the exact ground state energy, subject only to a fixed node approximation, and thus neatly complements the analytics. We use a variational wave function $\psi = e^{-J} D$ that is a product of a Slater determinant, D , that takes full account of the Fermion statistics, and a Jastrow factor J to include

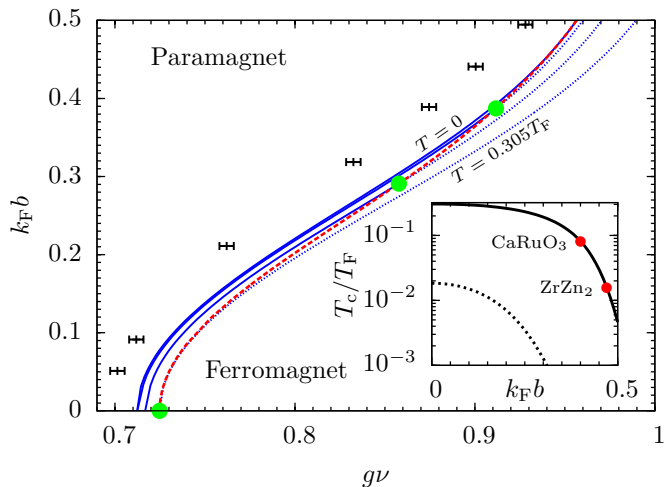


FIG. 1. (Color online): Phase boundaries at temperatures $T \in \{0, 0.1, 0.2, 0.305\}T_F$ with a screened Coulomb interaction of strength $g\nu$ and range $k_F b$. The ferromagnetic transition is first order (solid blue curves) at low $k_F b$, separated from the second order at larger $k_F b$ (dotted blue curves) by the green dots. The dashed red line is the locus of tricritical temperatures. The black points with error bars show the DMC $T = 0$ estimates for the phase boundary. The inset shows the tricritical temperature (solid black line) and the p-wave superconducting critical with $k_F b$, the red dots denote the CaRuO₃ family and ZrZn₂.

further correlations. We used a screened Coulomb repulsion $ge^{-r/b}/4\pi b^2 r$ that exactly reflects the potential used in the analytics.

The Slater determinant consists of plane-wave spinor orbitals containing both spin-up and spin-down electrons, $D = \det(\{\psi_{\mathbf{k} \in k_{F,\uparrow}}, \bar{\psi}_{\mathbf{k} \in k_{F,\downarrow}}\})$. Fixing the spin Fermi surfaces $\{k_{F,\uparrow}, k_{F,\downarrow}\}$ sets the magnetization. For computational efficiency we factorize the Slater determinant into an up and a down-spin determinant [37]. Provided that the orbitals of the minority spin state are the lowest energy orbitals of those in the majority spin state, [39], this gives the state whose total spin is S_{tot}^z .

The Jastrow factor, J , accounts for electron-electron correlations. It consists of the polynomial and plane-wave expansions in electron-electron separation proposed in Ref. [40]. To further optimize the wave function the orbitals in the Slater determinant were evaluated at quasi-particle positions related to the electrons through a polynomial backflow function [41] that partially relieves the fixed node approximation. The trial wave functions were optimized using QMC methods using VMC, backflow, and Diffusion Monte Carlo. Twist averaging was employed to remove finite size effects.

PHASE DIAGRAM

The analytical and computational tools developed calculate the free energy of the electron gas with screened Coulomb interaction. We seek the magnetization that minimizes the free energy to construct the phase diagram. To orient the discussion we first start with the common contact interaction at $k_F b = 0$. In Fig. 1 fluctuation corrections [15, 16] drive the transition first order at $g\nu \approx 0.7$ (versus the mean-field second order transition at $g\nu = 1$). The importance of fluctuations is reduced as we increase the temperature and ultimately the transition becomes second order at the tricritical temperature $T_c = 0.3T_F$. This tricritical point temperature is in agreement with previous studies of the contact interaction ([15, 16]) but is an order of magnitude higher than that seen in experiment.

At zero temperature, increasing the screening length diminishes the interaction strength for the fluctuation correction as $1/(1 + 4k_F^2 b^2)$ (Table (I)). With the driving force of the first order transition suppressed, the critical interaction strength rises towards the mean-field critical interaction strength $g\nu = 1$. Nevertheless, the transition remains resolutely first order due to a non-analytic contribution to the free energy of the form $M^4 \log(g^2 M^2 + T^2)$ [15]. However, with increasing $k_F b$ a slight temperature rise occludes the non-analyticity and the transition reverts to second order, exemplified in the inset of Fig. 1, which shows how the tricritical temperature rapidly reduces with rising screening length. Focusing on the CaRuO₃ family with $k_F b = 0.40$ [42] and ZrZn₂ with $k_F b = 0.47$ [43], the tricritical point temperature is reduced to $0.08T_F$ and $0.02T_F$ respectively with reasonable agreement to experiment [8, 9, 23].

We also study the magnetic transition at zero temperature using DMC. This predicts a phase boundary with increasing screening length that is quantitatively similar to the analytical predictions. Here the Monte Carlo is in better agreement with the analytical prediction compared with previous DMC studies [15, 34, 38] that employed a square potential with uncontrolled effective screening length.

A Landau expansion with the zero range system demonstrates that the first order ferromagnetic transition is always accompanied by a spin spiral phase [15, 22]. To incorporate the screening length we take the same Landau expansion [22], and rescale the interaction parameters according to Table (I). This reveals that the spiral phase persists in a thin strip of order $\Delta g\nu \approx 4 \times 10^{-4}$ between the first order phase boundary and the Lifshitz line, terminating at the tricritical point. The transition temperature of an instability to a p-wave superconductor was calculated by Ref. [22] and the associated interaction strengths can be rescaled following the prescription in Table (I). In the inset of Fig. 1 we find that the peak

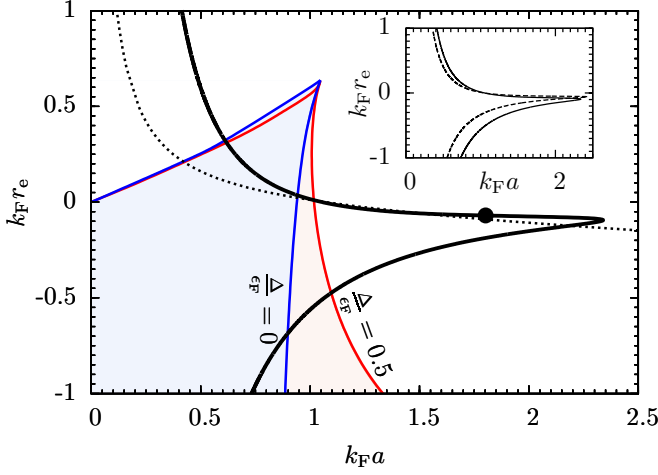


FIG. 2. (Color online) The phase diagram for a $T = 0$ cold atom gas with pseudopotential interaction strength $k_F a$ and effective range $k_F r_e$. The two shaded regions denote zero loss (shaded blue), and a loss rate less than $0.5\epsilon_F$ (shaded red). The thick black line represents the transition to the ferromagnetic state for the separable pseudopotential (whose fluctuation correction rescaling is zero at the black dot), and the dotted line the reciprocal pseudopotential transition. The inset compares the phase diagram for the full fluctuation corrections with separable pseudopotential (solid black line) to one obtained using the $g(\mathbf{p}, \mathbf{q}) \mapsto g(\sqrt{2}k_F, \sqrt{2}k_F)$ approximation (dashed black line).

superconducting transition drops with screening length even more rapidly than the tricritical temperature, obscuring the instability in typical materials.

Ultracold atomic gas

As in the solid state, finite range interactions alter the nature of the ferromagnetic transition. At zero effective range and zero temperature, the separable and reciprocal forms for the pseudopotential are identical so in Fig. 2 both magnetic transitions concur with previous studies that employed contact interactions [16, 25]. Sweeping the effective range through zero raises the rescaled interaction strength, reducing the critical interaction strength. At the negative effective range $k_F r_e = -1/8k_F a$, the scaling of the fluctuation term for the separable pseudopotential is zero, recovering the mean-field free energy for which the transition occurs at $k_F a = 5\pi/7$. At more negative effective range the fluctuation term is restored, thus reducing the critical interaction strength. In the case of the reciprocal pseudopotential, at large effective range the rescaled interaction strengths scale as $1/k_F r_e$, leading to a suppression of interaction effects and a quenching of the ferromagnetic transition at $k_F r_e \leq -0.68$. Although here the separable and reciprocal pseudopotentials lead to different phase behavior, this regime is not only beyond the effective range approximation where

higher order terms would be important, but furthermore in a regime where we will now determine that losses dominate.

In a cold atom gas, to generate the repulsive interaction experimentalists exploit a Feshbach resonance between the free atoms in the Fermi sea and the bound state of two atoms to generate a positive scattering length. However, as the bound state is necessarily lower in energy there is an instability to pair formation. The loss rate has been studied from both the paramagnetic [32] and polaronic [33] standpoints. To determine whether the ferromagnetic or pairing instability dominates, we follow Ref. [32] we start from Eqn. (2) and we decouple this interaction using a Hubbard-Stratonovich transformation into the Feshbach molecule channel $\Delta_{\mathbf{q}} = \sum_{\mathbf{k}} c_{\mathbf{k}\downarrow} c_{\mathbf{q}-\mathbf{k}\uparrow}$. At leading order the resulting Lagrangian is

$$|\Delta_{\omega, \mathbf{q}}|^2 \underbrace{\left(\frac{1}{g(\mathbf{0}, \mathbf{q})} + \int \frac{d^3 \mathbf{p}}{(2\pi)^3} \frac{n_F(\xi_{\mathbf{p}+\mathbf{q}/2\uparrow}) + n_F(\xi_{\mathbf{p}-\mathbf{q}/2\downarrow}) - 1}{i\omega - \xi_{\mathbf{p}+\mathbf{q}/2\uparrow} - \xi_{\mathbf{p}-\mathbf{q}/2\downarrow}} \right)}_{C^{-1}(\omega, \mathbf{q})}. \quad (4)$$

After regularizing the above integral [32], and specializing to an attractive potential with finite range r_e , we obtain an expression for the pairing susceptibility $C(\omega, \mathbf{q})$

$$\left[\frac{1}{g(\mathbf{0}, \mathbf{q})} + \frac{im}{4\pi} \sqrt{m \left(i\omega + 2\epsilon_F - \frac{q^2}{4m} \right)} - \frac{m^2 r_e}{8\pi} \left(i\omega + 2\epsilon_F - \frac{q^2}{4m} \right) + \int \frac{d^3 \mathbf{p}}{(2\pi)^3} \frac{n_F(\xi_{\mathbf{p}+\mathbf{q}/2\uparrow}) + n_F(\xi_{\mathbf{p}-\mathbf{q}/2\downarrow})}{i\omega - \xi_{\mathbf{p}+\mathbf{q}/2\uparrow} - \xi_{\mathbf{p}-\mathbf{q}/2\downarrow}} \right]^{-1}. \quad (5)$$

The imaginary component of the pairing susceptibility pole represents the bound state pairing rate. We find generally that the maximal pairing rate occurs for $\mathbf{q} = \mathbf{0}$.

In Fig. 2 we overlay the magnetic transition with lines of equal pairing rate Δ . Pairing rate reduces with increasing positive effective range as the molecules become more tightly bound. This leads to a window in the phase diagram where the system is both magnetized and there are no losses. However, at negative effective range the losses occur on a time-scale ~ 0.1 ms which is significantly shorter than the trap crossing time ~ 1 ms, so large magnetic domains cannot be formed. To date all Fermionic mixtures used in cold atom gas experiments have negative effective ranges so are not suitable for observing magnetic correlations [44], however a polar molecule gas with strong dipolar interactions does display large positive effective range [45] and a positive s -wave scattering length and so presents an opportunity to observe ferromagnetic phenomena.

The inset of Fig. 2 confirms that the phase boundary obtained by rescaling the interaction strength of the fluctuation contribution with the approximation $1 + 2ar_e(p^2 + q^2) \mapsto 1 + 8k_F a k_F r_e$ conforms with the phase boundary resulting from the exact momentum summation. This verifies the rescaling approximations given in Table (I).

DISCUSSION

The analytical fluctuation correction formalism with a contact repulsion has successfully demonstrated how quantum fluctuations drive not only a first order ferromagnetic transition, but also a spin spiral and a p-wave superconducting instability. The finite ranged interactions reduce the fluctuation corrections so dramatically suppress the tricritical point temperature from $0.3T_F$ to $0.02T_F$. This is quantitatively similar to the $T_c \approx 0.02T_F$ seen in $ZrZn_2$ [8, 9, 23]. Finite ranged interactions suppress the transverse magnetic fluctuations that occluded quantum criticality. With the tricritical temperature now reduced this system allows for the observation of quantum critical phenomena, such as those envisaged by Hertz.

The idealized Stoner Hamiltonian can also be studied in a cold atom gas. The positive effective finite range interaction, found in a polar molecular gas, eliminates the pairing permitting the observation of ferromagnetic order.

Acknowledgments: The authors are grateful to Stefan Baur, Andrew Green, Jesper Levinsen, Pietro Massignan, and Stephen Rowley for fruitful discussions. CVK acknowledges the financial support of the EPSRC, and GJC from Gonville & Caius College.

* gjc29@cam.ac.uk

- [1] J.A. Hertz, Phys. Rev. B **14**, 1165 (1976); A.J. Millis, Phys. Rev. B **48**, 7183 (1993); T. Moriya, Solid State Science **56** (Springer, Berlin, Heidelberg, 1985).
- [2] M. Uhlarz, C. Pfleiderer and S.M. Hayden, Phys. Rev. Lett. **93**, 256404 (2004).
- [3] A. Huxley, I. Sheikin and D. Braithwaite, Physica B **284-288**, 1277 (2000).
- [4] D.P. Rojas, J.I. Espeso, J.R. Fernández, J.C.G. Sal, C. Rusu, D. Andreica, R. Dudric, and A. Amato, Phys. Rev. B **84**, 024403 (2011).
- [5] C. Pfleiderer, S. Julian and G. Lonzarich, Nature (London), **414**, 427 (2001); W. Yu, F. Zamborszky, J.D. Thompson, J.L. Sarrao, M.E. Torelli, Z. Fisk and S.E. Brown, Phys. Rev. Lett. **92**, 086403 (2004).
- [6] M. Otero-Leal, F. Rivadulla, M. Garcia-Hernandez, A. Pineiro, V. Pardo, D. Baldomir and J. Rivas, arXiv:cond-mat/0806.2819v1 [cond-mat.str-el] (2008).
- [7] S. Lausberg, J. Spehling, A. Steppke, A. Jesche, H. Luetkens, A. Amato, C. Baines, C. Krellner, M. Brando, C. Geibel, H.-H. Klauss, and F. Steglich, arXiv:1210.5463.
- [8] R. Borzi, S. Grigera, J. Farrell, R. Perry, S. Lister, S. Lee, D. Tennant, Y. Maeno and A.P. Mackenzie, Science **315**, 214 (2007).
- [9] W. Wu, A. McCollam, S.A. Grigera, R.S. Perry, A.P. Mackenzie, and S.R. Julian, Phys. Rev. B **83**, 045106 (2011).
- [10] A. Huxley, I. Sheikin, E. Ressouche, N. Kernavanois, D. Braithwaite, R. Calemczuk and J. Flouquet, Phys. Rev. B **63**, 144519 (2001).
- [11] S. Watanabe and K. Miyake, J. Phys. Chem. Solids **63**, 1465 (2002).
- [12] S.S. Saxena, P. Agarwal, K. Ahilan, F.M. Grosche, R.K.W. Haselwimmer, M.J. Steiner, E. Pugh, I.R. Walker, S.R. Julian, P. Monthoux, G.G. Lonzarich, A. Huxley, I. Sheikin, D. Braithwaite and J. Flouquet, Nature (London) **406**, 587 (2000).
- [13] D. Aoki, A. Huxley, E. Ressouche, D. Braithwaite, J. Floquet, J.-P. Brison, E. Lhotel, and C. Paulsen, Nature (London) **413**, 613 (2001).
- [14] N.T. Huy, A. Gasparini, D.E. de Nijs, Y. Huang, J.C.P. Klaasse, T. Gortenmulder, A. de Visser, A. Hamann, T. Görlach, and H.v. Löhneysen, Phys. Rev. Lett. **99**, 067006 (2007).
- [15] G.J. Conduit, A.G. Green and B.D. Simons, Phys. Rev. Lett. **103**, 207201 (2009).
- [16] G.J. Conduit and B.D. Simons, Phys. Rev. A **79**, 053606 (2009).
- [17] D. Belitz, T. R. Kirkpatrick, and T. Vojta, Physical Review B **55**, 9452 (1997).
- [18] D. V. Efremov, J. J. Betouras, and A. Chubukov, Physical Review B **77**, (2008).
- [19] D. L. Maslov and A. V. Chubukov, Physical Review B **79**, 075112 (2009).
- [20] J. Rech, C. Pepin, and A. V. Chubukov, Physical Review B **74**, (2006).
- [21] T. R. Kirkpatrick and D. Belitz, Physical Review B **85**, (2012).
- [22] G.J. Conduit, C.J. Pedder, and A.G. Green, submitted to Phys. Rev. Lett.
- [23] J. Hooper, Z. Mao, R. Perry, and Y. Maeno, Phys. Rev. Lett. **92**, 257206 (2004).
- [24] G.-B. Jo *et al.*, Science **325**, 1521 (2009).
- [25] G.J. Conduit and B.D. Simons, Phys. Rev. Lett. **103**, 200403 (2009).
- [26] G.J. Conduit and E. Altman, Phys. Rev. A **82**, 043603 (2010).
- [27] G.J. Conduit, Phys. Rev. A **82**, 043604 (2010).
- [28] C.W. von Keyserlingk and G.J. Conduit, Phys. Rev. A **83**, 053625 (2011).
- [29] P. Massignan and G.M. Bruun, Eur. Phys. J. D **65**, 83 (2011).
- [30] R.A. Duine and A.H. MacDonald, Phys. Rev. Lett. **95**, 230403 (2005).
- [31] D. Pekker *et al.*, Phys. Rev. Lett. **106**, 050402 (2011).
- [32] D. Pekker and E. Demler, e-print arXiv:1107.3930v1.
- [33] C. Kohstall, M. Zaccanti, M. Jag, A. Trenkwalder, P. Massignan, G.M. Bruun, F. Schreck, and R. Grimm, Nature **485**, 615 (2012).
- [34] S. Pilati, G. Bertaina, S. Giorgini and M. Troyer, Phys. Rev. Lett. **105**, 030405 (2010); S.-Y. Chang, M. Randeria and N. Trivedi, Proceedings of the National Academy of Sciences **108**, 51 (2011).
- [35] C. Pethick and H. Smith, Bose-Einstein condensation in dilute gases. Cambridge University Press (2002).
- [36] D.R. Phillips, S.R. Beane, and T.D. Cohen, Annals of Physics, **263**(2), 255 (1998).
- [37] R.J. Needs, M.D. Towler, N.D. Drummond, and P. López Ríos, J. Phys.: Condensed Matter **22**, 023201 (2010).
- [38] D.M. Ceperley and B.J. Alder, Phys. Rev. Lett. **45**, 566 (1980); G. Ortiz, M. Harris, and P. Ballone, **82**, 5317

- (1999); F.H. Zong, C. Lin, and D.M. Ceperley, Phys. Rev. E **66**, 036703 (2002).
- [39] C.C.J. Roothaan, Rev. Mod. Phys. **32**, 179 (1960).
- [40] N.D. Drummond, M.D. Towler and R.J. Needs, Phys. Rev. B **70**, 235119 (2004).
- [41] P. López Ríos, A. Ma, N.D. Drummond, M.D. Towler and R.J. Needs, Phys. Rev. E **74**, 066701 (2006).
- [42] I.I. Mazin and D.J. Singh, Phys. Rev. Lett. **79**, 733 (1997).
- [43] G. Santi1, S.B. Dugdale and T. Jarlborg, Phys. Rev. Lett. **87**, 247004 (2001).
- [44] C. Chin, R. Grimm, P S. Julianne, and E. Tiesinga, Rev. Mod. Phys. **82**, 1225 (2010).
- [45] Z.-Y. Shi, R. Qi, and H. Zhai, Phys. Rev. A **85**, 020702 (2012).